JACS
JOURNAL OF THE AMERICAN CHEMICAL SOCIETY
Article
pubs.acs.org/JACS

Isolating the Effects of the Proton Tunneling Distance on Proton-Coupled Electron Transfer in a Series of Homologous Tyrosine-Base Model Compounds

Starla D. Glover,[#] Giovanny A. Parada,[†,#] Todd F. Markle,[†] Sascha Ott,[*] and Leif Hammarström[*]

Department of Chemistry—Ångström, Uppsala University, Box 532, SE-751 20, Uppsala, Sweden

Supporting Information

ABSTRACT: The distance dependence of concerted proton-coupled electron transfer (PCET) reactions was probed in a series of three new compounds, where a phenol is covalently bridged by a 5, 6, or 7 membered carbocycle to the quinoline. The carbocycle bridge enforces the change in distance between the phenol oxygen (proton donor) and quinoline nitrogen (proton acceptor), $d_{O\cdots N}$, giving rise to values ranging from 2.567 to 2.8487 Å, and resulting in calculated proton tunneling distances, r_0, that span 0.719 to 1.244 Å. Not only does this series significantly extend the range of distances that has been previously accessible for experimental distance dependent PCET studies of synthetic model compounds, but it also greatly improves the isolation of $d_{O\cdots N}$ as a variable compared to earlier reports. Rates of PCET were determined by time-resolved optical spectroscopy with flash-quench generated $[Ru(bpy)_3]^{3+}$ and $[Ru(dce)_3]^{3+}$, where bpy = 2,2′-bipyridyl and dce = 4,4′-dicarboxyethylester-2,2′-bipyridyl. The rates increased as $d_{O\cdots N}$ decreased, as can be expected from a static proton tunneling model. An exponential attenuation of the PCET rate constant was found: $k_{PCET}(d) = k^0_{PCET}\exp[-\beta(d - d_0)]$, with $\beta \sim 10$ Å^{-1}. The observed kinetic isotope effect (KIE = k_H/k_D) ranged from 1.2 to 1.4, where the KIE was observed to *decrease* slightly with increasing $d_{O\cdots N}$. Both β and KIE values are significantly smaller than what is predicted by a static proton tunneling model. We conclude that vibrational compression of the tunneling distances, as well as higher vibronic transitions, that contribute to concerted proton coupled electron transfer must also be considered.

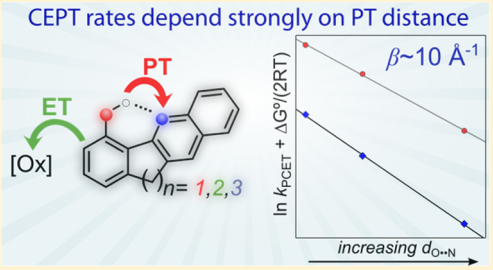

INTRODUCTION

Proton-coupled electron transfer (PCET) reactions are gaining broad recognition for their role in biological and molecular catalytic transformations.[1−5] The role of PCET in enzyme driven catalysis has for example been discussed in detail for photosystem II,[6−8] ribonucleotide reductase,[9−11] cytochrome c oxidase,[12,13] photolyase,[14,15] and lipoxygenase.[16−18] PCET reactions have also been investigated in the context of biomimetic[19,20] and organometallic catalysis.[21−24] A full kinetic and mechanistic description of PCET processes in biological and chemical systems not only poses an exciting challenge, but also stands to provide a picture of the basic chemical requirements necessary to design better catalytic systems. Model systems that are simplified in structure, in that they contain only the active chemical components necessary for PCET, can be useful in obtaining detailed information about the fundamental properties that govern these reactions, while minimizing complexity that would need to be managed in the study of natural systems. Of particular interest are PCET studies that have focused on systems modeled after the tyrosine-histidine pair in Photosystem II.[8,25−36] These model compounds contain phenol, the proton and electron donating functional group of tyrosine, and a covalently bound base that acts as proton acceptor. Investigations of phenol-base model systems have advanced our general understanding about the different mechanistic pathways of PCET, energetic factors and the effect of hydrogen bonding to a proton acceptor.

The electron and proton transfer distances are also expected to affect PCET rates, yet a very limited number of experimental studies have specifically addressed this in synthetic systems. Recently Wenger and co-workers have reported on the role of *electron* transfer distance dependence in PCET reactions,[33,37] while the distance dependence of *proton* transfer on concerted PCET reactions was experimentally addressed in separate studies by the groups of Hammarström and Mayer.[31,32,38,39] Hammes-Schiffer and co-workers have computationally examined the proton-transfer distance dependence in enzymes, models systems and proton reduction catalysts.[2,5,40] A direct experimental comparison between the proton tunneling distance and kinetics of PCET is challenging because of the short distances over which a proton can tunnel, typically 1 Å or much less, and it is difficult to vary proton tunneling distances by several 0.1's of an Å while keeping constant other parameters that affect PCET rates. In this article we present new phenol-base model compounds which have been designed to minimize electronic and energetic differences through the series while varying the proton transfer distance; this will make

Received: December 5, 2016
Published: January 4, 2017

DOI: 10.1021/jacs.6b12531
J. Am. Chem. Soc. 2017, 139, 2090−2101

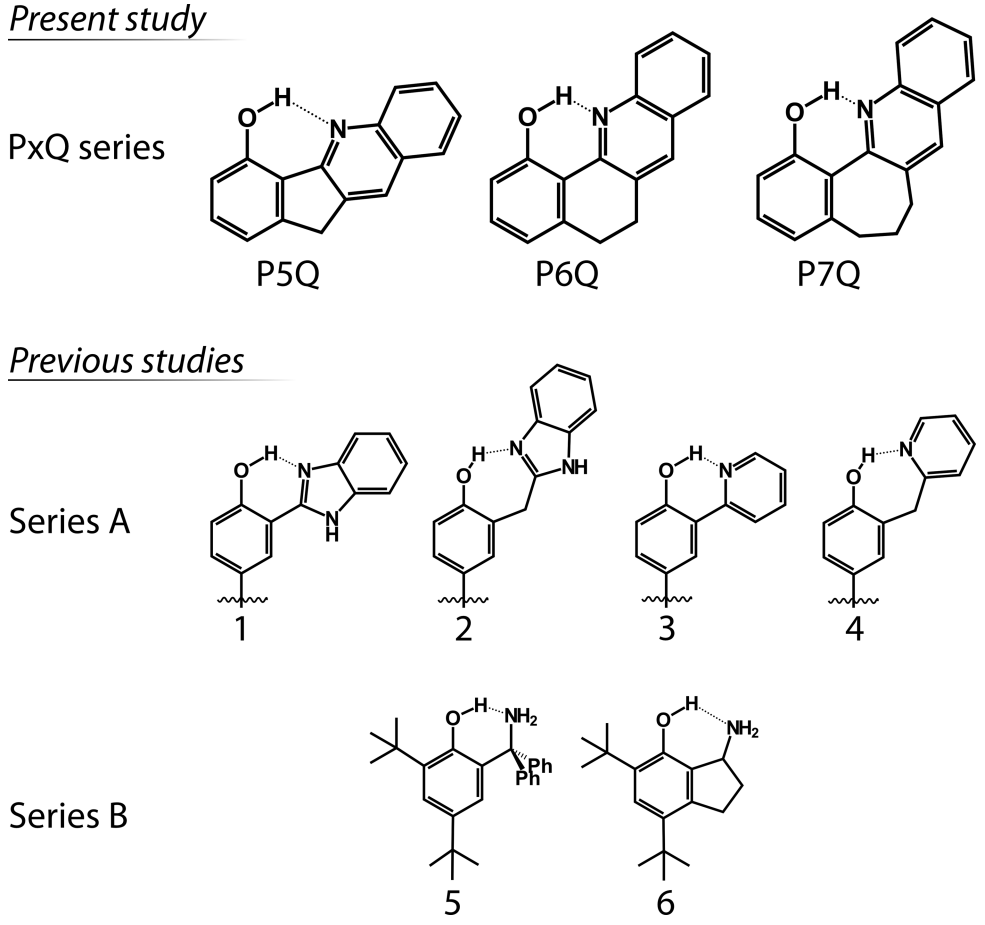

Figure 1. Top: Structures of the PxQ series of compounds used to probe the rates of proton coupled electron transfer as a function of proton donor−acceptor distance. Bottom: Compounds previously used to probe the proton donor−acceptor distance dependence on CEPT. In series A the oxidant was a covalently linked ruthenium tris-bipyridyl derivative while series B used several outer-sphere oxidants.

for a more direct evaluation of the effect of proton tunneling distance on PCET.

The proton donor−acceptor distance ($d_{O\cdots N}$), which is presently defined as the distance between the phenol oxygen and basic nitrogen proton, can provide a reasonable metric for the proton tunneling distance, r_0, which is the distance of proton displacement during the PCET reaction. Though r_0 is much shorter than $d_{O\cdots N}$, variations of these values are expected to track each other well (vide infra). The aforementioned studies by Hammarström and Mayer and co-workers, where concerted electron proton transfer (CEPT) was investigated as a function of proton donor−acceptor distance, employed compounds having a phenol as the proton and electron donor and a covalently linked base as the proton acceptor (Figure 1).[31,32] In series A (Figure 1) $d_{O\cdots N}$ was varied by either changing the type of base or by the addition of a methylene unit in the covalent linkage.[31] The two complexes in series B (Figure 1) varied $d_{O\cdots N}$ by introducing a different functionality to the carbon linking the phenol and amine.[32] Despite the similar motifs between series A and B, the two systems displayed very different trends in CEPT rates as a function of $d_{O\cdots N}$.

In the case of series A, the variation in $d_{O\cdots N}$ values was 0.185 Å and gave rate constants for CEPT spanning 2 orders of magnitude at a comparable driving force. The nonconjugated variants (**2** and **4**) with greater $d_{O\cdots N}$ values exhibited much slower CEPT rate constants despite having ∼0.2 eV more favorable ΔG°. Within this series a strong distance dependence of CEPT was demonstrated; the rate constants displayed an exponential decrease with distance (as defined in eq 1 below) with a characteristic decay parameter reported as $\beta = 27$ Å^{-1},[31] later corrected to 33 Å^{-1} due to a revised $d_{O\cdots N}$ value for one compound.[39]

$$k_{PCET}(d_{O\cdots N}) = k^0{}_{PCET}\exp[-\beta(d_{O\cdots N} - d^0{}_{O\cdots N})] \quad (1)$$

The β-value agreed well with theoretical predictions for a static proton tunneling model of CEPT, i.e., assuming that the proton transfer distance for each compound is fixed at the respective equilibrium value, and that only vibronic ground state transitions are involved[41,42] (vide infra).

In the case of series B, $d_{O\cdots N}$ varied by 0.165 Å, but when both compounds were studied under similar driving force conditions the CEPT rate constants differed by only a factor of ca. 2, which is a much smaller difference than would be predicted from a static tunneling model. An analysis of proton vibrational wave functions suggested that higher vibronic transitions were likely involved in CEPT and that predictions from a static tunneling model do not necessarily hold.

The contrasting behavior in series A versus B makes it difficult to delineate how changing the proton tunneling distance affects CEPT rate constants. First, it is not straightforward to quantify to what extent conjugation versus nonconjugation between the proton donating group and proton accepting group influenced CEPT in series A.[39] The

DOI: 10.1021/jacs.6b12531
J. Am. Chem. Soc. 2017, 139, 2090−2101

degree of conjugation may potentially influence not only ΔG°_{PCET} but also the electronic coupling (V_{ET}), reorganization energy (λ) and compressibility of the O···N distance (see Theoretical Background). Furthermore, changing the identity of the proton accepting base or altering functional groups in the proton donor and acceptor subunits will result in changes to ΔpK_a through the series, which is expected to introduce differences in the proton transfer free energy profiles that are not only due to donor−acceptor distances. In an effort to more effectively isolate the proton donor−acceptor distance from the complications outlined above, we have designed the series of three new phenol-quinoline compounds shown in Figure 1 (top).

Our goal with the new series is to vary the proton donor−acceptor distance while minimizing other structural, energetic and electronic changes that affect the classical reaction barrier or the proton transfer reaction coordinate. Design features for such a series of compounds would: (*i*) maintain the same conjugation pattern between phenol−OH donor and accepting base, (*ii*) use identical proton donor and acceptor functional groups and, (*iii*) introduce a systematic variation in the distance between proton donor and acceptor units. Meeting design goals *i* and *ii* will ensure similar electronic character in the phenolic donor and minimize differences in pK_a between proton donor and acceptor units through the series. Thus, changes in ΔG^0, λ and V_{ET} are minimized while $d_{O\cdots N}$ is varied.

The series of three new compounds each possess a phenol (P) to which a quinoline (Q) is covalently bound in the *ortho* position. The difference between the three phenol-quinoline compounds arises from the incorporation of one to three methylene units that link the meta-phenol and meta-*N*-quinoline carbons forming a carbocycle of increasing ring size. The choice of a quinoline group as base was for synthetic reasons, allowing for formation of the pyridine via a condensation reaction.[43] The nomenclature for the compounds in the PxQ series is as follows: P5Q, P6Q, and P7Q species bear a 5, 6, and 7-membered carbocycle, respectively. The change in $d_{O\cdots N}$ in the PxQ series is effectuated by the size and conformational preference of the carbocycle bridge between the phenol and quinoline units.

The synthesis and structural characterization of this new phenol-quinoline series has been reported separately.[43,44] Here we have used X-ray crystallography, DFT, electrochemistry, NMR, and transient spectroscopic measurements to quantify the proton transfer coordinate structure as well as the thermodynamics and kinetics associated with PCET for the PxQ series. We found that the proton donor−acceptor distance as a variable was well isolated from other relevant parameters in this series where large differences in conjugation and donor−acceptor pK_a were avoided. A very strong correlation between the proton donor−acceptor distance and CEPT rate constants was demonstrated for the PxQ series.

THEORETICAL BACKGROUND

Proton-coupled electron transfer reactions can be broadly defined as processes that involve the movement of both protons and electrons. In multisite PCET reactions the electron and proton does not originate from the same donor and/or transfer to the same acceptor. For example, the system in this study undergoes multisite PCET wherein the electron is transferred to an external oxidant and the proton is transferred to a covalently linked base. In the present case, PCET is also called bidirectional, a term that often overlaps with "multisite" but is not by definition synonymous. Instead, "bidirectional" emphasizes the electrostatic polarization, which is central to Marcus theory, and which is very different from that of a unidirectional PCET where the charge neutral hydrogen atom transfer (HAT) is the extreme case. An illustrative example is the self-exchange PCET between phenol and phenoxyl radical, which is clearly unidirectional, but multisite (and not HAT) because the electron is transferred between π-orbitals while the proton is transferred between σ-orbitals.[45,46]

Hammes-Schiffer, Soudackov and co-workers have developed theory based on the electron transfer theory of Marcus[47,48] and proton transfer theory of Hynes[49−51] to reconcile coupled proton and electron movement.[2,52] In this model the transferring protons and electrons are treated quantum mechanically while other nuclei in the system are treated classically. Concerted proton-coupled electron transfer (CEPT) can be understood as a "double tunneling" reaction where proton and electron tunnel to the product state via the same transition state without formation of intermediates.

CEPT can be described as a vibronic transition between reactant (μ) and product (ν) states where CEPT rates depend on the Boltzmann distribution of reactant states (P_μ), the vibronic coupling matrix element, $V_{\mu\nu}$, the total reorganization energy (λ), and the reaction driving force ($\Delta G_{\mu\nu}^{\circ}$). The rate expression for CEPT is then given by the equation below.[2,5]

$$k_{PCET} = \sum_{\mu} P_\mu \sum_{\nu} \frac{|V_{\mu\nu}|^2}{\hbar}\sqrt{\frac{\pi}{\lambda k_B T}}\exp\left\{-\frac{(\Delta G_{\mu\nu}^{\circ} + \lambda)^2}{4\lambda k_B T}\right\} \quad (2)$$

Typically $V_{\mu\nu}$ is taken to equal the product of the electronic coupling, V_{ET}, and the Franck−Condon overlap between reactant and product proton vibrational wave functions, $S_{\mu\nu}$, such that $V_{\mu\nu} = V_{ET}S_{\mu\nu}$.[2,5] The V_{ET} and $S_{\mu\nu}$ terms will each have a dependence on the donor−acceptor distance for electron and proton transfer, respectively, where shorter distances generally lead to greater wave function overlap. The inverse relationship, where $S_{\mu\nu}$ increases with distance has also been predicted for systems in which higher vibronic transitions contribute to CEPT.[38] Protons having a much greater mass than electrons exhibit more localized wave functions, therefore proton tunneling should have a greater sensitivity to distance than electron tunneling. This has been observed experimentally where electrons tunnel over very long distances[37,53−55] (tens of Å) while protons are expected to tunnel over much shorter distances, typically less than 1 Å. In the electronically nonadiabatic limit for proton transfer the vibronic coupling as a function of donor−acceptor distance, $d_{O\cdots N}$, takes the form,[56]

$$V_{\mu\nu}(d_{O\cdots N}) = V_{ET}S_{\mu\nu}(d_{O\cdots N}) \quad (3a)$$

The overlap parameter $S_{\mu\nu}$ can be approximated to decrease exponentially as a function of distance when $d_{O\cdots N}$ is near the equilibrium value $d^0_{O\cdots N}$ as given by

$$S_{\mu\nu} = S^0_{\mu\nu}\exp\left\{-\frac{\beta}{2}(d_{O\cdots N} - d^0_{O\cdots N})\right\} \quad (3b)$$

where $S^0_{\mu\nu}$ is the overlap at the equilibrium distance, and β (the attenuation parameter that appears in eq 1) describes the exponential decay of the overlap near the equilibrium distance.[56] The distance dependence of the vibronic coupling can then be expressed by eq 3c.

$$V_{\mu\nu}(d_{O\cdots N}) = V_{ET}S^0_{\mu\nu}\exp\left\{-\frac{\beta}{2}(d_{O\cdots N} - d^0_{O\cdots N})\right\} \quad (3c)$$

DOI: 10.1021/jacs.6b12531
J. Am. Chem. Soc. 2017, 139, 2090−2101

Eq 1, which relates k_{PCET} as a function of $d_{O\cdots N}$, is derived from eq 3c and the relationship that $k_{PCET} \propto V_{\mu\nu}^2$ (from eq 2).

Eqs 3a−3c could describe variations in coupling due to vibrational (thermal) compression of $d_{O\cdots N}$ from the equilibrium value $d^0_{O\cdots N}$ in a single compound,[30,57,58] or variations in equilibrium value for a series of related compounds. In the latter case $d^0_{O\cdots N}$ is an arbitrarily chosen reference distance for which $S_{\mu\nu} = S^0_{\mu\nu}$, and $k_{PCET} = k^0_{PCET}$. For static tunneling reactions β values associated with proton transfer are predicted to range from ca. 25 to 50 $Å^{-1}$;[41,46] this is a much steeper exponential dependence on distance than for electron transfer reactions which typically have β values around 1 $Å^{-1}$ or less.[53,55,59] From a theoretical perspective, the proton tunneling distance is expected to be a key parameter in determining rates of CEPT.

RESULTS AND DISCUSSION

PCET in the PxQ series is a multisite process where the electron is transferred intermolecularly to the oxidant and the proton is transferred intramolecularly to the nitrogen on the quinoline (Scheme 1). PCET will occur when these

Scheme 1. Representation of the PCET Reaction in the PxQ Series

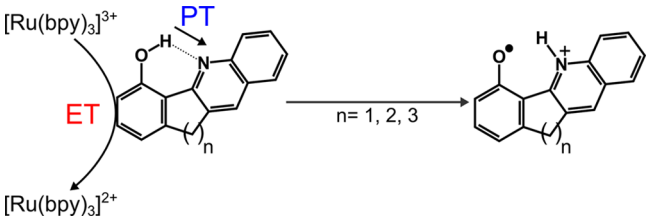

compounds form an activated complex with a photogenerated external oxidant. Our investigations are carried out in acetonitrile solution, unless otherwise noted, and the oxidant is laser flash-quench generated $[Ru(bpy)_3]^{3+}$ or $[Ru(dce)_3]^{3+}$ (vide infra), where bpy = 2,2′-bipyridyl and dce = 4,4′-dicarboxyethylester-2,2′-bipyridyl. PCET can take place as a concerted electron−proton transfer (CEPT) reaction or it can proceed in a stepwise fashion where electron transfer precedes proton transfer (ETPT) or electron transfer follows proton transfer (PTET). The concerted pathway is often favored because it avoids endergonic steps to the high energy intermediates, specifically, a deprotonated reduced phenoxide resulting from PT or the protonated oxidized phenol cation resulting from ET. By thermodynamic and kinetic arguments we show that PCET proceeds in a concerted mechanism where electron and proton are transferred in a single kinetic step (vide infra).

We begin with a description of the proton transfer coordinate in the PxQ series, followed by results from electrochemical and kinetic measurements. Using structural, thermodynamic and kinetic data for the series, we then interpret the proton transfer distance dependence of CEPT.

The Proton Transfer Coordinate. ^{1}H NMR spectroscopy, as well as crystallographic and structural DFT calculations all provide information about the proton transfer coordinate. ^{1}H NMR will report on the stereoelectronic environment of phenolic protons in the PxQ series. ^{1}H NMR spectra for the PxQ series have been reported separately[43] and here we summarize the chemical shift values of relevance. The chemical shifts are nearly invariant within the PxQ series, with the exception of the phenolic −OH proton. These protons display significantly different chemical shifts relative to each other; for P5Q, P6Q, and P7Q values of 9.85, 14.69, and 11.75 ppm were observed, respectively. Compared to unfunctionalized phenol the PxQ phenolic proton experiences a strong downfield shift due to participation in a hydrogen bond to the quinoline nitrogen. Interestingly, despite the high degree of structural similarity of P5Q, P6Q and P7Q, the chemical shifts of the phenolic protons within this series vary by almost 5 ppm, which indicates that the strength of the O−H···N hydrogen bonding interaction varies significantly between these three compounds. Given that the functional groups participating in the hydrogen bond are identical, the difference in chemical shifts of the phenolic protons in the PxQ series must arise from changes in the hydrogen bond geometry imposed by the bridge. A shorter distance to the nitrogen allows for a stronger O−H···N hydrogen bonding interaction and greater desheilding of the proton. From the ^{1}H NMR spectra it can be predicted that $d_{O\cdots N}$ increases through the series as follows: P6Q < P7Q < P5Q.

The room temperature ^{1}H NMR spectrum for P5Q displayed a broadened phenolic resonance peak indicative of exchange. This was not the case with P6Q and P7Q whose spectra showed a sharp peak for the phenolic proton. A series of temperature dependent spectra ranging from 238 to 298 K revealed that the P5Q proton can exchange with trace water present in acetonitrile-d_3. Exchange correlation spectroscopy (EXSY)[60] showed that P5Q exchanges with water at 320 s^{-1}. This is far too slow to influence PCET kinetics in the present study; the observed rate constants in transient absorption experiments (vide infra) gave values which were ca. 3 orders of magnitude faster than exchange with water. The series of temperature dependent ^{1}H NMR spectra and the EXSY spectrum are given in the Supporting Information in Figures S1 and S2.

A geometric description of the proton transfer coordinate and specifically values of $d_{O\cdots N}$ can be determined from X-ray crystallographic and DFT structures. Crystal structures were obtained for all molecules of the PxQ series and the structural details have been reported.[43,44] We found very good agreement between DFT (specifically B3LYP/6-31G(d,p) with a polarizable continuum model of acetonitrile solvent) and X-ray crystallographic structures of P5Q, P6Q, P7Q, particularly with respect to the bond angles and distances about the proton transfer coordinate, which are critical for the description of $d_{O\cdots N}$ and r_0 (Figure 2a). Relevant geometric coordinates are summarized in Table 1.

In each structure there is a clear O−H···N hydrogen bonding interaction where $d_{O\cdots N}$ values span a range of 0.282 Å, from 2.567 to 2.8487 Å. The carbocycle tether not only affects $d_{O\cdots N}$, but flexibility in the 2- and 3-carbon tethers also affects the dihedral angle between the phenol and quinoline units about the sp^2-hybridized C−C link. As the number of carbons in the tether increases, the dihedral angle between phenol and quinoline units increases. P5Q is coplanar while P6Q has a small dihedral angle of 11.7°. P7Q, with the longest carbocycle tether gives the largest dihedral angle of the series at 33.1°.

The proton donor−acceptor distance, $d_{O\cdots N}$, is a convenient metric for the proton-tunneling distance in that it can be readily determined crystallographically or by DFT calculations of the reactant species. The proton tunneling distance (r_0), defined as the difference in the equilibrium distance of the proton position before and after the double tunneling event (Figure 2a),

DOI: 10.1021/jacs.6b12531
J. Am. Chem. Soc. 2017, 139, 2090−2101

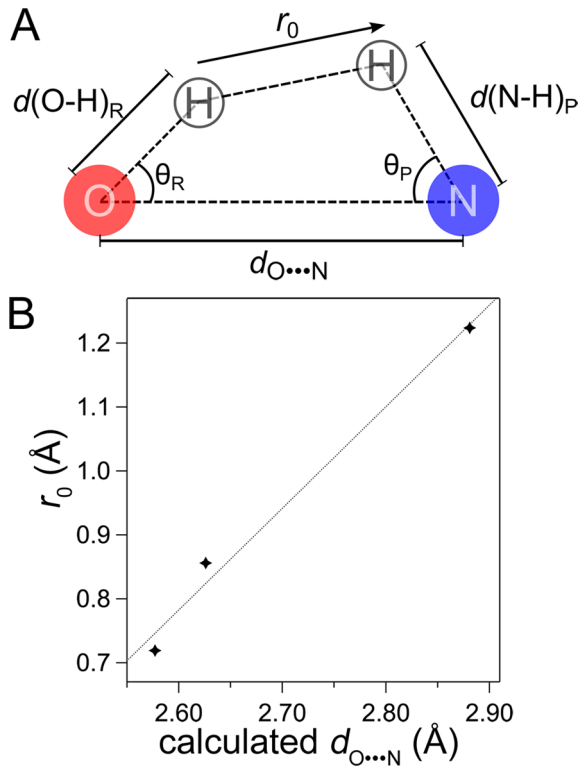

Figure 2. (a) Scheme of geometries used to calculate $d_{O\cdots N}$ and r_0 distances. (b) Plot of proton tunneling distances (r_0) versus proton donor−acceptor ($d_{O\cdots N}$) from DFT. The linear fit gave a slope of 1.6 and an R^2 value of 0.987.

requires coordinates for the product structure. Values of r_0 were estimated from optimized DFT structures of the reduced (OH-bound) reactant and oxidized (NH-bound) forms of the PxQ series. Plotting r_0 as a function of calculated $d_{O\cdots N}$ shows a strong linear correlation (Figure 2b). From X-ray crystallographic and calculated structures of the PxQ series it can be seen that $d_{O\cdots N}$ increases with the same trend as predicted from the ^{1}H NMR spectra; i.e., $d_{O\cdots N}$ increases as such, P6Q < P7Q < P5Q. Values for $d_{O\cdots N}$ and r_0 are given in Table 1.

A linear fitting to the data in Figure 2b gave a slope of 1.6 and R^2 value of 0.987. A slope greater than one is simply an effect of the increasing $d_{O\cdots N}$ and θ_R and θ_P. The strong hydrogen bond interaction in P6Q pulls the proton toward the nitrogen (in the reduced neutral form) or the oxygen (in the oxidized cation form), which serves to decrease θ_R and θ_P, respectively (Figure 2b). Increasing $d_{O\cdots N}$ in P7Q and P5Q weakens the hydrogen bond and allows the proton to pull away from its hydrogen-bond partner. This has the effect of increasing θ_R and θ_P making the hydrogen bond less linear. The effect of increasing $d_{O\cdots N}$ as well as θ_R and θ_P leads to an increase of r_0 such that the slope of r_0 as a function of $d_{O\cdots N}$ is greater than 1. It should be stated that values for r_0 are estimates, as isolation of the N−H bound cation is not feasible experimentally. Nonetheless, the strong correlation between r_0 and $d_{O\cdots N}$ is encouraging for the analysis of rates and distance for this series. It is also noteworthy that the range of $d_{O\cdots N}$ and r_0 values accessed by the PxQ series has been significantly extended in comparison to the previously studied Series A. Specifically, the $\Delta d_{O\cdots N}$ and Δr_0 values for the PxQ series are 0.282 and 0.5 Å, respectively, while for Series A they are 0.185 and 0.21 Å, respectively.[31,39]

We stress that $d_{O\cdots N}$ and r_0 are calculated from static equilibrium structures. Solution phase systems will of course be subject to vibrational fluctuations that modulate $d_{O\cdots N}$ and r_0 about an equilibrium value. Vibrational compression can increase overlap between reactant and product states and has been suggested to enhance PCET rates.[16,30,40,58,61−65] We revisit this concept for the PxQ series below.

Reduction Potentials for PxQ. We expect the PxQ series to be electronically similar given that the proton donor and proton acceptor are the same and the conjugation pattern bridging them is identical. This similar electronic and steric character through the series should lead to similar electrochemical potentials and by extension, similar PCET driving forces. The PCET reaction driving force in units of eV is given by $-\Delta G^\circ_{PCET} = e[E^\circ(Ru^{III/II}) - E^\circ(P^\bullet xQH^+/PxQ)]$, where e is the elementary electron charge, $E^\circ(Ru^{III/II})$ is the $Ru(bpy)_3^{3+}/Ru(bpy)_3^{2+}$ redox couple of the external oxidant and $E^\circ(P^\bullet xQH^+/PxQ)$ refers to the redox couple associated with PxQ oxidation. The reduction potential, $E^\circ(P^\bullet xQH^+/PxQ)$, was determined by cyclic voltammetry and details describing the electrochemical methods are given in the Supporting Information. $E^\circ(Ru^{III/II})$ values are taken from literature[66] and are 0.890 and 1.14 V vs ferrocene/ferrocenium[67] for $[Ru(bpy)_3]^{2+/3+}$ and $[Ru(dce)_3]^{2+/3+}$, respectively. Values for E° and ΔG°_{PCET} for the PxQ series are given in Table 1.

We found that $E^\circ(P^\bullet xQH^+/PxQ)$ values vary less than 30 mV through the series. This change is very small, and the differences in E° are consistent with the overall structural, electronic and steric similarities of the compounds. We attribute the small increase in $E^\circ(P^\bullet xQH^+/PxQ)$ to the increase in dihedral angle between donor and acceptor units. Though the PxQ series has the same conjugation pattern

Table 1. Summary of Structural and Thermodynamic Parameters for the PxQ Series[a]

	P5Q		P6Q		P7Q	
	(XRD)[b]	DFT	(XRD)[c]	DFT	(XRD)[c]	DFT
$d_{O\cdots N}$ (Å)	2.8487(5)	2.881	2.567(2)	2.577	2.666(1)	2.626
r_0 (Å)	–	1.244	–	0.719	–	0.856
dihedral angle (deg)	2.81(1)	0.01	−12.9	−11.7	−36.2	−33.1
δ (ppm)	8.91		14.69		11.75	
E° (V vs $FeCp_2^{+/0}$)	0.747		0.756		0.773	
$-\Delta G_{PCET}^\circ$ ($[Ru(bpy)_3]^{3+}$)	0.143		0.134		0.117	
$-\Delta G_{PCET}^\circ$ ($[Ru(dce)_3]^{3+}$)	0.393		0.384		0.367	

[a]Crystallographic values are reported to the first standard deviation (given in parentheses). r_0 values were estimated from DFT calculations. ^{1}H NMR spectra and chemical shift values have been reported separately. Values for ΔG° are given in units of eV. [b]Value from ref 43. [c]Value from ref 44.

DOI: 10.1021/jacs.6b12531
J. Am. Chem. Soc. 2017, 139, 2090−2101

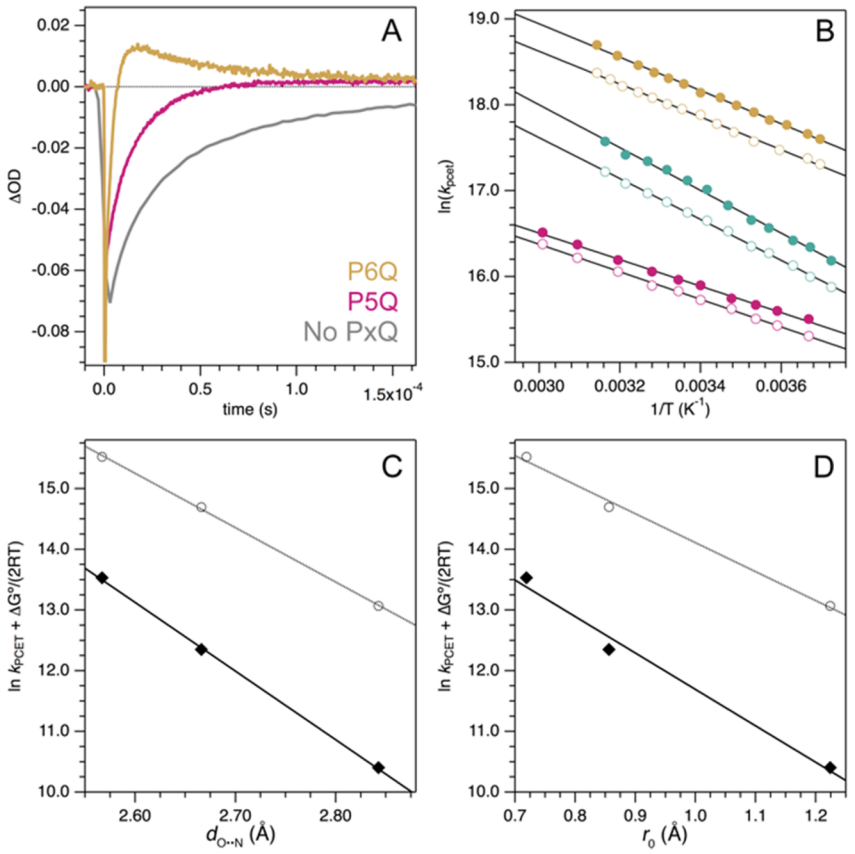

Figure 3. (a) Kinetic traces recorded at 450 nm that follow the recovery of $[Ru(bpy)_3]^{2+}$ after laser flash-quench oxidation, in the presence of 5 mM P6Q (yellow) yellow), 5 mM P5Q (magenta) and the absence of PxQ substrate (gray). Solvent: acetonitrile. The kinetic traces for solutions containing PxQ substrate exhibit accelerated decay due to PCET (eq 6). (b) ln (k_{pcet}) plotted as a function of temperature for P5Q (magenta), P6Q (yellow) and P7Q (green). Filled and open circles correspond to samples where proton transfer or deuteron transfer was studied, respectively. (c) PCET rate constants corrected for differences in ΔG° plotted as a function of $d_{O\cdots N}$ (from XRD). R^2 values of 0.9994 and 0.9996 were obtained for linear fits to $[Ru(bpy)_3]^{2+}$ and $[Ru(dce)_3]^{2+}$ data, respectively. (d) PCET rate constants corrected for differences in ΔG° plotted as a function of the proton tunneling distance, r_0, determined from DFT. R^2 values of 0.995 and 0.993 for $[Ru(bpy)_3]^{2+}$ and $[Ru(dce)_3]^{2+}$, respectively In panels (c) and (d) filled diamonds (◆) correspond to CEPT with $[Ru(dce)_3]^{3+}$ oxidant in 1:1 acetonitrile/*n*-butyronitrile solvent system while unfilled circles (○) correspond to CEPT with $[Ru(bpy)_3]^{3+}$ oxidant in acetonitrile.

between proton donor and proton acceptor groups, the increasing dihedral angle will present a slight decrease in conjugation through the series. The trend in dihedral angles mirrors that of $E^{\circ}(P^{\bullet}xQH^{+}/PxQ)$ suggesting that a more planar structure will be better able to stabilize the charge and unpaired spin of the oxidized product via resonance, therby lowering $E^{\circ}(P^{\bullet}xQH^{+}/PxQ)$. We emphasize that the electronic changes due to differences in conjugation in the PxQ series must be small as demonstrated by the similarity in reduction potentials. This means also that ΔG°_{PCET} and ΔpK_a are well conserved in this series. By the structural and electrochemical investigation of the PxQ series we have thus found well-defined distance parameters that have significant $\Delta d_{O\cdots N}$ and Δr_0 while differences in driving force are minimized.

Transient Absorption Spectroscopy for PCET Kinetics. Rates of PCET in the PxQ series were obtained by transient absorption (TA) measurements that were carried out in a fashion similar to previous flash-quench photolysis experiments reported by our group.[31,68] A 7 ns laser flash triggered the excitation of $[Ru(bpy)_3]^{2+}$, to give ~15 μM of *$[Ru(bpy)_3]2+$ (eq 4) that was quenched by methyl viologen (40 mM $MV(PF_6)_2$, denoted MV^{2+}) with $\tau \sim 150$ ns leading to the generation of ca. 5 μM each of $[Ru(bpy)_3]^{3+}$ and $MV^{+\bullet}$ (eq 5). Subsequent oxidation of PxQ by $[Ru(bpy)_3]^{3+}$ led to an intermolecular ET/intramolecular PT, which constitutes the PCET reaction (eq 6). PxQ concentrations used in kinetic investigations ranged from 0.1−5 mM, which is in large excess of $[Ru(bpy)_3]^{3+}$. The recovery of $[Ru(bpy)_3]^{2+}$ (eq 6) is expected to proceed by pseudo-first-order kinetics where kinetic traces can be fit to single exponential decays to obtain the observed rate constant, k_{obs}. eqs 7 and 8 are the recombination reactions that regenerate the reactants. When the oxidized $P^{\bullet}xQH^{+}$ encounters $MV^{+\bullet}$, PxQ reactant and MV^{2+} are regenerated (eq 8). Lastly, the radical phenol-quinoline species that is formed from the PCET reaction can dimerize (eq 9). We found that changes in [PxQ] due to dimerization were not significant; samples having been subject to upward of 10^3 laser flashes gave identical kinetic response to freshly prepared samples. This served as a verification that the changes in [PxQ] due to dimerization, were insignificant in these kinetic measurements.

$$[Ru(bpy)_3]^{2+} \xrightarrow{h\nu} *[Ru(bpy)_3]^{2+} \quad (4)$$

$$*[Ru(bpy)3]^{2+} + MV^{2+} \rightarrow [Ru(bpy)_3]^{3+} + MV^{+\bullet} \quad (5)$$

DOI: 10.1021/jacs.6b12531
J. Am. Chem. Soc. 2017, 139, 2090−2101

Table 2. Summary of Experimentally Determined PCET Kinetic Parameters[a]

	P5Q	P6Q	P7Q	$\beta(d_{O\cdots N})(R^2)$[a]	$\beta(r_0)$ (R^2)[b]
[c]$k_{PCET}/10^7$ $M^{-1}s^{-1}$)					
$[Ru(bpy)_3]^{3+}$	0.795	7.76	2.43	7.5 (0.9994)	4.8 (0.995)
$[Ru(dce)_3]^{3+}$	7.70	147	31.9	9.4 (0.9996)	6.0 (0.993)
[d]E_a (H)	12.8 ± 0.2	16.1 ± 0.3	17.1 ± 0.4		
[d]E_a (D)	13.3 ± 0.6	15.9 ± 0.2	20.8 ± 0.7		
[d]ΔE_a	0.5 ± 0.6	−0.2 ± 0.4	3.7 ± 0.8		
[d]ln A (H)	21.1 ± 0.1	24.8 ± 0.1	24.6 ± 0.3		
[d]ln A (D)	21.2 ± 0.2	24.4 ± 0.1	25.7 ± 0.3		
[e]KIE	1.17 ± 0.02	1.40 ± 0.04	1.35 ± 0.01		

[a]Exponential decay parameter for k_{PCET} as a function of $d_{O\cdots N}$ in units of $Å^{-1}$ from a fit to the data according to eq 11 (R^2 in parentheses). [b]Exponential decay parameter for k_{PCET} as a function of r_0 in units of $Å^{-1}$ (R^2 in parentheses). [c]k_{PCET} with $[Ru(bpy)_3]^{3+}$ and $[Ru(dce)_3]^{3+}$ as oxidant, respectively, reported with a standard deviation of ±10%. [d]Arrhenius parameters E_a and ln A from the analysis of temperature dependent k_{PCET} values with $[Ru(bpy)_3]^{3+}$ as oxidant and with ΔE_a defined as $E_a(D)$-$E_a(H)$. [e]KIE values with $[Ru(bpy)_3]^{3+}$ as oxidant.

$$[Ru(bpy)_3]^{3+} + PxQ \underset{k_{-d}}{\overset{k_d}{\rightleftharpoons}} [[Ru(bpy)_3]^{3+}\cdots PxQ] \xrightarrow{PCET} [Ru(bpy)_3]^{2+} + P^{\bullet}xQH^{+} \quad (6)$$

$$[Ru(bpy)_3]^{3+} + MV^{+\bullet} \rightarrow [Ru(bpy)_3]^{2+} + MV^{2+} \quad (7)$$

$$P^{\bullet}xQH^{+} + MV^{+\bullet} \rightarrow PxQ + MV^{2+} \quad (8)$$

$$2P^{\bullet}xQH^{+} \rightarrow \text{dimer} \quad (9)$$

The observed PCET reactions are much slower than diffusion controlled processes which occur with rates of ca. 10^{10} M^{-1} s^{-1}. PCET rate constants were therefore determined by the relationship for an activation controlled reaction: $k_{obs} = K_d k_{PCET}[PxQ]$, where K_d describes the ratio of diffusion and dissociation rate constants, k_d and k_{-d}, respectively (eq 6), which gives k_{PCET} in units of M^{-1} s^{-1}. From our data, K_d and k_{PCET} cannot be determined independently, but given the similarity of the compounds under study here it is reasonable to assume that K_d is nearly constant through the series. As the purpose is to study the variation in rate with distance, the relative values of k_{PCET}, and not the absolute values, are of importance here. For simplicity we therefore assume that K_d = 1, giving $k_{obs} = k_{PCET}[PxQ]$.

When the pseudo-first order rate constant k_{obs} is small, $[Ru(bpy)_3]^{2+}$ can also be regenerated through competitive electron transfer from $MV^{+\bullet}$ to $[Ru(bpy)_3]^{3+}$ (eq 7). In these cases, k_{obs} values were obtained from a modified fit routine that accounted for this competitive recombination. Details of this fit routine are given in the Supporting Information. We found that the need to correct for competitive recombination could be avoided in most experiments by maintaining higher PxQ concentrations, in the mM range; however, because of the intrinsically slower PCET rate constant in P5Q, all kinetic traces recorded for P5Q where $[Ru(bpy)_3]^{3+}$ was the oxidant needed to be corrected for competitive recombination.

Figure 3a shows kinetic traces collected at 450 nm, that track the recovery of $[Ru(bpy)_3]^{2+}$ in three different samples: a sample containing 5 mM P6Q, a sample containing 5 mM P5Q, and a sample containing only $[Ru(bpy)_3]^{2+}$ and MV^{2+}. The trace corresponding to the sample that does not contain PxQ substrate, shown in gray (Figure 3a), follows the recovery of $[Ru(bpy)_3]^{2+}$ as it recombines with $MV^{+\bullet}$. This decay obeys second-order kinetics, as expected for a bimolecular reaction with $[Ru^{III}] = [MV^{+\bullet}]$ (eq 7). The sample with 5 mM P5Q, shown in magenta (Figure 3a), shows accelerated recovery at 450 nm versus the sample with no PxQ substrate. This faster Ru^{III}-to-Ru^{II} recovery is due to electron transfer from P5Q to $[Ru(bpy)_3]^{3+}$ as in eq 6. Thus, this trace follows the PCET kinetics where intermolecular electron transfer from P5Q to $[Ru(bpy)_3]^{3+}$ is accompanied by intramolecular proton transfer from phenol oxygen to quinoline nitrogen. The yellow trace corresponds to a solution containing 5 mM P6Q and shows faster recovery than the sample containing the same molar concentration of P5Q. Again, this accelerated recovery is due to the PCET reaction wherein P6Q transfers an electron to $[Ru(bpy)_3]^{3+}$. The traces from samples with P5Q and P6Q also show a positive signal after decay. This positive signal is due to the absorbance of $MV^{+\bullet}$ still present in the solution on the time scale of the measurement, and which decays according to eqs 7 and 8. The higher positive ΔOD at earlier times for the sample of P6Q is observed because more rapid PCET contributes to faster decay of the negative signal while at the same time more $MV^{+\bullet}$ remains present in solution because the possibility to recombine with $[Ru(bpy)_3]^{3+}$ has been diminished. Formation of the phenoxy radical could not be directly demonstrated as its signal (ε_{410} = 3000 M^{-1} cm^{-1}) is covered by the much stronger absorbance of $MV^{+\bullet}$ (ε_{396} = 40 000 M^{-1} cm^{-1}).[25] This is a general problem with acceptors suitable for rapid flash-quench oxidation of Ru^{II} complexes in organic solvent. Nevertheless, the strongly accelerated Ru^{III} reduction in the presence of PxQ is clear evidence for PxQ oxidation.

Since [P5Q] and [P6Q] are equal for the kinetic traces in Figure 3a the observed pseudo-first-order rate constants can be directly compared. The trace corresponding to the P6Q sample gave a k_{obs} approximately ten times faster than the sample of P5Q. ΔG°_{PCET} values for PCET in P5Q and P6Q are nearly identical, differing only by ca. 0.03 eV, while $d_{O\cdots N}$ is 0.282 Å longer in P5Q than P6Q. Considering the similarity of the P5Q and P6Q systems as a whole; e.g., ΔG°_{PCET}, solvent, [PxQ], and temperature, the significantly faster k_{obs} in P6Q must originate from the much shorter $d_{O\cdots N}$ in P6Q. It was not possible to obtain a trace for P7Q at 5 mM concentration for direct comparison of traces in Figure 3a, as this compound has a lower solubility in acetonitrile as compared to P5Q and P6Q. At lower concentrations the second order rate constant for P7Q was determined, and was found to be about three times larger than P5Q and three times smaller than P6Q.

DOI: 10.1021/jacs.6b12531
J. Am. Chem. Soc. 2017, 139, 2090−2101

PCET kinetics for P5Q, P6Q and P7Q were recorded under two different driving force conditions using photogenerated $[Ru(bpy)_3]^{3+}$ and $[Ru(dce)_3]^{3+}$. We consistently observed that for the PxQ series, PCET rate constants decreased as r_0 and $d_{O\cdots N}$ increased. This trend can be seen clearly in Figures 3c and 3d that plot rates as a function of $d_{O\cdots N}$ by XRD and r_0, respectively. To compensate for the small variation in driving force within the PxQ series the PCET rates were extrapolated to their predicted values at $\Delta G^\circ_{PCET} = 0$, using the linear correlation in eq 10 which is the partial derivative of eq 2:

$$\frac{\delta \ln k_{PCET}}{\delta \Delta G^\circ_{PCET}} = -\frac{1}{2RT}\left(1 + \frac{\Delta G^\circ_{PCET}}{\lambda}\right) \tag{10}$$

We assume that $-\Delta G^\circ \ll \lambda$, so that ln k_{PCET} varies by one logarithmic unit per 50 meV in ΔG°, which is a well-known result from the Marcus theory of electron transfer.[47,48] The linear fits follow eq 11 below, and the slope of the line gives β of eq 2. This formulation has been used previously.[31,39] Slopes and corresponding R^2 values are given in Table 2.

$$\ln k_{PCET} + \frac{\Delta G^\circ_{PCET}}{2RT} = -\beta d_{O\cdots N} + \text{constant} \tag{11}$$

An excellent linear correlation between PCET rate constants and the two proton transfer distance parameters, r_0 and calculated $d_{O\cdots N}$, was found for the PxQ series under both oxidant conditions. CEPT rate constants in Figures 3c and 3d were estimated at the limit of $\Delta G^\circ = 0$, and ideally the rates for PxQ series with each oxidant would be expected to overlay each other. However, when $[Ru(dce)_3]^{3+}$ is used as the oxidant PCET is faster and has a larger driving force, but eq 11 slightly overcorrects these rate constants. This does not present an issue with our interpretation as the most valuable information obtained from these correlation plots is the value for β. The values for β agree very well for the two different oxidant conditions, which serves as an indication that the correction does not interfere with the correlation of rates to $d_{O\cdots N}$ and r_0. We found that the correlation between rate and distance was quite satisfactory also in the absence of the $\Delta G^\circ/2RT$ correction factor, where values of $R^2 > 0.96$, and that β values were also very similar. Thus, we can confidently say that our interpretation of the distance dependence of PCET rates will be the same whether or not the correction factor is implemented. For the interested reader, additional plots correlating k_{PCET} to $d_{O\cdots N}$, r_0, and δ(OH) are given in the Supporting Information in Figure S4.

PCET rate constants for reactions of the PxQ series with $[Ru(bpy)_3]^{3+}$ were also measured as a function of temperature and H/D-isotope. The proton on the phenolic oxygen is readily exchanged in the presence of excess protons or deuterons supplied by H_2O or D_2O (1−2% in acetonitrile). Isotopic substitution with deuterons at the phenolic oxygen site was achieved by working in the presence of a ca. 500-fold excess of deuterons. In the interest of keeping reaction conditions as similar as possible for the two different isotopes, proteo transfer was also studied in the presence of the same molar excess of protons. The same rate was observed for PCET with and without the excess proton source, demonstrating that exchange with 1−2% water did not in any way obscure PCET kinetics. Figure 3b shows the temperature dependence of k_{PCET} for P5Q, P6Q and P7Q under proton and deuteron transfer conditions. The Arrhenius equation, $k_{PCET} = A\exp(-E_a/RT)$, was assumed for the linear fits to temperature dependent data. Values for the activation energies and preexponential terms and KIEs for the PxQ series are reported in Table 2.

Mechanism for PCET. The kinetic and thermodynamic information gathered for the PxQ series can be used to distinguish the mechanism by which PCET proceeds. Either PCET occurs in a concerted fashion, where the proton and electron transfer occurs by a double tunneling mechanism in a single kinetic step (CEPT), or by one of two stepwise mechanisms. The stepwise pathways are PTET, where a proton transfer (PT) precedes electron transfer (ET), or ETPT where proton transfer occurs after electron transfer. Both stepwise pathways involve the formation of high energy intermediates, specifically the zwitterionic P^-xQH^+ species of the PTET pathway (Figure 4, top) and oxidized protonated phenoxyl

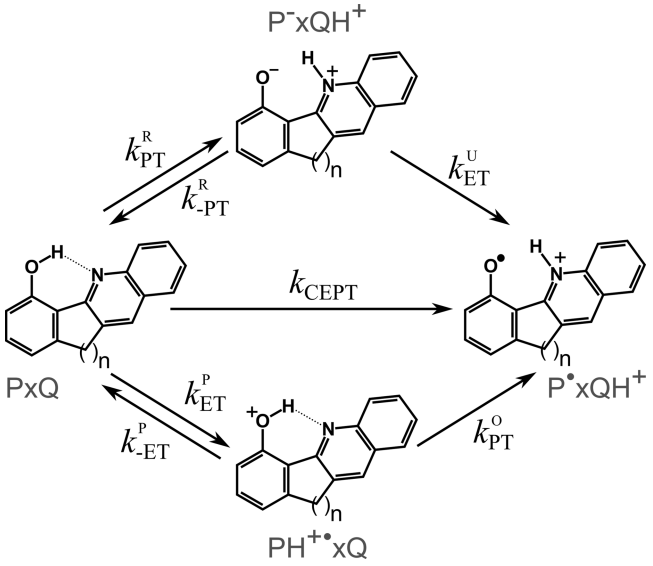

Figure 4. Mechanistic pathways for PCET in the PxQ series. Electron transfer to the external oxidant is presumed to occur via an enounter complex where $K_d \approx 1$ as in eq 6, vide supra. The superscripts R, O, P and U denote whether the phenol is reduced, oxidized, protonated, or unprotonated, respectively during proton transfer (PT) or electron transfer (ET).

radical, $PH^{+\bullet}xQ$ of the ETPT pathway (Figure 4, bottom). We breifly describe below why the formation of these high energy intermediates under our experimental conditions is disfavored, making CEPT the operative mechanism in the PxQ series.

The general rate expressions for stepwise PTET and ETPT mechanisms under a steady-state approximation for the intermediate are given in eqs 12 and 13, respectively.[2] The PT and ET subscripts denote proton and electron transfer, respectively while the superscript denotes whether the phenol donor is reduced (R) or oxidized (O) and protonated (P) or unprotonated (U). Contributions to the overall rate contants given in eqs 12 and 13 can be traced to the relevant individual steps of Figure 4.

$$k_{PTET} = k^R_{PT}\frac{k^U_{ET}}{(k^U_{ET} + k^R_{-PT})} \tag{12}$$

$$k_{ETPT} = k^P_{ET}\frac{k^\circ_{PT}}{(k^\circ_{PT} + k^P_{-ET})} \tag{13}$$

Suitable conditions for PTET are met if proton transfer is either rate-limiting or if PT occurs under favorable pre-equilibrium

DOI: 10.1021/jacs.6b12531
J. Am. Chem. Soc. 2017, 139, 2090−2101

conditions. However, a pre-equilibrium PT is disfavored on the basis of a very small PT equilibrium constant for the PxQ series, where k_{PT} is estimated to be ca. 10^{-15}, based on the pK_a values of phenol (27) and quinoline (ca. 12).[69−72] This would imply that the unimolecular follow-up ET in the encounter/successor complex needs to be unphysically rapid, $k_{ET}^{U} = 10^{21}$ M^{-1} s^{-1} or faster, to match the PCET rate constants observed here. Using a more conservative estimate of k_{PT} = ca. 10^{-4} from DFT calculated values[44] (Supporting Information), indicates that bimolecular electron transfer from the keto-form would have to occur with $k_{ET}^{U} = 10^{11}$ M^{-1} s^{-1} to match the observed value with P6Q and $[Ru(bpy)_3]^{3+}$, which is still above the diffusion limit.

In a rate limited PT reaction the follow up ET in the encounter complex must be significantly faster than reverse proton transfer ($k_{ET}^{U} \gg k_{-PT}^{R}$). PT to form the $P^{-}xQH^{+}$ zwitterion is expected to be endergonic implying that reverse PT will be highly favorable such that k_{-PT}^{R} in the encounter complex is equal to the frequency factor from absolute rate theory, 6×10^{12} s^{-1}.[73] This means that the unimolecular follow up electron transfer in the encounter/successor complex would need to proceed even faster, which is unlikely for an electronically nonadiabatic system. Therefore, rate limiting PT can also be eliminated as a possible mechanism.

ETPT can occur either by rate limiting ET or by preequilibrium ET where both mechanisms involve the formation of an oxidized protonated phenol, $P^{+\bullet}HxQ$. However, based on electrochemical data for the anisole analogues of P5Q and P6Q, electron transfer is significantly uphill: ΔG_{ET}^{0} = +33 and +30 kJ mol^{-1}, respectively (Supporting Information), and because of the similarity between the compounds, the value for P7Q should be similar. This is significantly higher than the observed experimental activiation energies (13−16 kJ mol^{-1}, Table 2), which excludes a pre-equilibrium ETPT mechanism. Also rate limiting ET can be excluded, as there is no real (i.e., nonimaginary) value of the reorganization energy (λ) within Marcus theory (eq 14)[47,48] for which ΔG°_{ET} = +30 kJ mol^{-1} can give an activation energy as low as the experimental value of 16 kJ mol^{-1} (i.e., $\Delta G^{\circ}_{ET} > E_a$; see Supporting Information). Moreover, the observed relative rates for P5Q and P6Q is a factor of 10, while eq 14 with $\Delta\Delta G_{ET}^{0}$ = 3 kJ mol^{-1} would predict factor of only ∼2.

rate-limiting ET:

$$k_{ETPT} = k_{ET}^{P} = A\exp\left[\frac{-(\Delta G^{\circ}_{ET} + \lambda_{ET})^2}{4\lambda_{ET}RT}\right] \quad (14)$$

To summarize, both ETPT and PTET mechanisms would require unrealistic kinetics from individual ET or PT steps and/or the formation of intermediates that are too high in energy. Therefore, we confidently assign a concerted mechanism for PCET in the PxQ system. We think it is of interest to note that it has been suggested that for strongly hydrogen bonded phenol-base systems a concerted electron and proton transfer is the only viable mechanism, owing to the inability to identify vibronic states corresponding to the stepwise intermediates.[38]

Interpreting the Distance Dependence of CEPT. The most direct strategy to delineate how changing the proton tunneling distance affects CEPT is to minimize the difference in other parameters that contribute to CEPT while changing the proton donor−acceptor distance (see eq 1). It seems that the PxQ system has largely satisfied this requirement in terms of ΔG°, λ, and V_{ET}; ΔG° varies less than 30 meV in the PxQ series, and the high degree of similarity in size, shape and structure of the series suggests that changes in λ and electronic coupling should be small. Consequently, the change in relative CEPT rate constants in the PxQ series is expected to originate primarily from the differences in reactant and product proton wave function overlaps, $S_{\mu\nu}$, between the compounds in the series. As mentioned above, $S_{\mu\nu}$ is a function of proton donor−acceptor distance and will be affected both by changing the equilibrium distance within a series of similar compounds and by molecular vibrations that modulate the proton transfer distance in a each compound. The experimental studies performed thus far address the differences in equilibrium proton donor−acceptor distances for the PxQ series. Presently, we utilize what is known about equilibrium proton-donor−acceptor distances for the PxQ system in conjuction with kinetic data (KIE, β, and Arrhenius parameters) to describe CEPT.

We first compare our kinetic results with the predictions of a static proton tunneling model, i.e., a model where the proton donor−acceptor distance $d_{O\cdots N}$ is assumed to be fixed in each individual compound, and the proton potential is nearly harmonic (a Morse potential with large dissociation energy). In this model, and with a small driving force as in the present experiments, $S_{\mu\nu}$ is dominated by contributions from ground vibronic states ($\mu = \nu = 0$); therefore, very large β values are predicted, on the order of 25 $Å^{-1}$ or greater.[41,46] KIE values are also predicted to be large (>2) and should increase as $d_{O\cdots N}$ increases.[56] Both trends in β and KIE arise from changes in $S_{\mu\nu}$. For β the strong attenuation of rates originates from a steep decrease in overlap of reactant and product wave functions as the equilibrium $d_{O\cdots N}$ distance increases. The increase in KIE arises from the fact that deuterium has more localized wave functions; this means that reactant-product overlap for deuterium experiences greater attenuation as a function of distance than does a proton. Thus, at longer distances, the difference in rates between proton and deuteron transfer will be greater and a larger KIE is predicted.[56]

The kinetic behavior in the PxQ system, however, does not reflect behavior consistent with such a static tunneling model. The β values in terms of $d_{O\cdots N}$ and r_0 for the PxQ system were 7.5−9.4 and 4.8−6.0 $Å^{-1}$, respectively, which is much smaller than the predicted values. In addition, KIEs were found to decrease as a function of increasing proton donor−acceptor distance, which is opposite of the predicted trend. As a static proton tunneling model does not capture the kinetic trends as a fuction of distance, we next consider a dynamic proton tunneling model, often attributed to Kuznetsov and Ulstrup,[74] which takes into consideration molecular vibrations that affect $d_{O\cdots N}$ and thus the proton vibrational wave function overlap ($S_{\mu\nu}$).

Molecular vibrations that act upon the proton transfer coordinate lead to a thermal distribution of donor−acceptor distances. The reactivity is much higher at short distances, so that the thermal distribution increases the average $S_{\mu\nu}$ compared to its value at the equilibrium $d_{O\cdots N}$, and thus this "vibrational enhancement" leads to a higher observed k_{PCET}.[30,63,75] The fraction of compounds with a short distance increases with temperature, which gives an addition to the experimental activation energy for PCET. Accelerated PCET rates as well as temperature dependent,[16,76] moderate,[30] and inverse[77] KIEs have all been correlated with vibrational enhancement. Here we focus on the trend in activation energies for the PxQ series where E_a values for the PxQ series

DOI: 10.1021/jacs.6b12531
J. Am. Chem. Soc. 2017, 139, 2090−2101

were determined by Arrhenius analysis of CEPT rates as a function of temperature (Figure 3b and Table 2).

First, we note than an upper estimate of the reorganization energy $\lambda \leq 0.9$ eV can be made from the values of E_a and ΔG° for P6Q(H) using a classical barrier model ($E_a = \Delta G^{\ddagger} = (\Delta G^\circ + \lambda)^2/4\lambda$).[47,48] However, this limit assumes no contributions to E_a from vibrational compression or higher vibronic transitions, or from the encounter complex formation in eq 6 (i.e., $\Delta H^0_{encounter} \sim 0$). We cannot quantitatively disentangle these contributions to E_a, but it is likey that $\lambda < 0.9$ eV.

Second, variations in E_a were indeed observed for the PxQ series. The difference in E_a between compounds in the PxQ series is not likely to originate primarily from changes in the classical barrier,, based on the similarity in ΔG° and expected λ for the series. Instead, the trends in k_{PCET}, KIE, and E_a for P6Q and P7Q are qualitatively as expected for a PCET reaction that is modulated by vibrational enhancement. P7Q has a longer r_0 and is therefore more susceptible to vibrational enhancement, and the higher values of E_a and ΔE_a reflect the increased average compression of the O−N distance, in particular for the deuterated compound.[30] With a shorter r_0, P6Q is predicted to have a smaller E_a and ΔE_a, which correctly reflects the trend predicted for vibrationally enhanced rates. Vibrational enhancement is also expected to decrease the β-value compared to the value of ≥ 25 Å^{-1} predictied by static tunneling model, as is indeed observed for the PxQ series.

P5Q is instead a clear outlier for this model with the longest r_0 and smallest k_{PCET}, and yet the smallest KIE and E_a; vibrational enhancement should leave P5Q with the largest E_a of the series, and still a higher KIE than for the other compounds. What can explain the different behavior for P5Q? First, it is important to point out that k_{PCET} is still the smallest in the series even though the activation energy is the smallest, thus the proton tunneling probablility is clearly an important important factor, even if the KIE is small. One effect that could contribute to the results for P5Q is that the effective force constant (κ) is predicted to be smaller for the vibrations that modulate $d_{O\cdots N}$, which would facilitate compression and increase k_{PCET} relative to the other compounds (Figure S5).[32,38,39] Another effect is that multiple vibronic transitions may contribute to CEPT, and the weight of a given vibronic transition is determined by the proton vibrational wave function overlap and the splitting between energy levels.[38,56]

DFT has been useful in predicting donor and acceptor wave function and overlaps in model systems,[56] some of which are closely related to compounds **3**−**5** and the PxQ series (Figure 1).[38,78] The following qualitative trends found from the DFT studies can help explain the kinetic observations for the PxQ series: (*i*) transitions from reactant ground state to excited product vibronic states were found to significantly contribute to CEPT, i.e., overlap integrals $S_{\mu\nu}$, where $\mu,\nu \geq 1$, were significant and in several instances contributed more to the total overlap than S_{00};[38,40,65,78,79] (*ii*) longer proton donor−acceptor distances tended to show increased relative contributions from higher vibronic transitions to CEPT.[38,78] This was augmented by the fact that the proton potentials are often much more anharmonic than the Morse potential used in the Ulstrup-Kuznetzov model, and the anharmonicity is often greater at larger $d_{O\cdots N}$.[38,65,78] Consequently, the energies of the higher vibrational states are lower and their wave functions are more delocalized, which may substantially increase their contribution to the overall rate; (*iii*) subtitution with deuterium also tended to increase the contribution from higher vibronic transitions, which can be explained by the smaller splittings between vibrational energy levels for deuterium;[38,78] and (*iv*) the force constant κ of vibrations that modulate the proton donor−acceptor distance generally decrease as the equilibrium distance increases, because steric repulsion makes it harder to compress $d_{O\cdots N}$ as the equilibrium distance decreases.[38,39]

The small β value for this series can be rationalized by the effect of vibrational enhancement, with additional contributions from the effects of trends *i*, *ii* and *iv*. Since excited state proton wave functions are more diffuse than those of the ground state, vibronic transitions through excited states would relax the distance dependence of proton tunneling as compared to a static, $\mu = 0 \rightarrow \nu = 0$ proton tunneling. This would result in CEPT rates that do not depend as strongly on distance and in turn β values would be smaller.

Trends *ii*, *iii* and *iv* may help explaining why the KIE for P5Q is the smallest in the series. KIEs are proportional to $|S_{\mu\nu}(H)|^2/|S_{\mu\nu}(D)|^2$, or the ratio of the square of proton and deuterium wave function overlaps.[56] Our KIE data suggest that for P5Q, with the longest $d_{O\cdots N}$, $|S_{\mu\nu}(H)|^2$ and $|S_{\mu\nu}(D)|^2$ factors become more similar than for the other compounds in the PxQ series. The improvement in overlap when deuterium tunnels via higher vibronic states will compensate for the reduced overlap from deuterium having more localized wave functions. Since both increased distance and deuteron transfer favor tunneling involving higher vibronic excited states, this effect should become more pronounced with increased distance which can result in $|S_{\mu\nu}(H)|^2$ and $|S_{\mu\nu}(D)|^2$ factors becoming more similar. Trend *iv* on the other hand suggests that it may be easier to thermally compress $d_{O\cdots N}$ from its equilibrium value in P5Q, which facilitates tunneling also via vibrational ground states. The combined effects of trend *iv* and trends *ii*−*iii* can contribute to P5Q having a negligible KIE, compared to the modest but significant KIEs for P6Q and P7Q. With these suggested explanations, it is important to also note that the activation energy for k_{PCET} is the smallest in P5Q. Both contributions of vibrational enhancement (related to κ) and excited reactant vibronic states ($\mu > 0$) are activated processes, and would increase the activation energy for P5Q, in apparent contradiction to what is observed in the experiments. However, both contributions are most likely active also for P6Q and P7Q, as is clear from the modest KIE and β-values. As the compressed $d_{O\cdots N}$'s and excited vibronic states are less activated in P5Q, the observed activation energy can still be smaller than for the other compounds.

Looking at the PxQ series as a whole, the distance dependent kinetic data (KIE, β, and Arrhenius parameters) suggest that both vibrational enhancement and excited state vibronic transitions are important for CEPT. Further elucidation on the proton tunneling character of CEPT may be accessible by experimental and computational studies that further address CEPT activity as a function of both temperature and pressure-induced compression along the proton transfer coordinate. Along these lines the PxQ series provides key insights given the consitency of ΔG°_{PCET} and λ and V_{ET} for the three compounds.

CONCLUSIONS

We have presented the first series of synthetic compounds for PCET studies in which the proton-transfer distance could be systematically varied while other structural, energetic and electronic factors remained essentially constant. This makes the PxQ series very well suited for a study of the effect of proton tunneling distance on CEPT with $d_{O\cdots N}$ well isolated as a

DOI: 10.1021/jacs.6b12531
J. Am. Chem. Soc. 2017, 139, 2090−2101

variable. A very strong correlation between CEPT rate constants and proton donor−acceptor distance and proton tunneling distance was clearly demonstrated with the PxQ series. This shows that the proton tunneling probablility is an important factor influencing k_{PCET} in this series, even though the KIE values are modest.

We found that CEPT rate constants versus distance followed the intuitive trend that would be predicted from a static tunneling model involving ground state $\mu = 0$ to $\nu = 0$ vibronic transitions; i.e., as $d_{O\cdots N}$ and r_0 increase rate constants for CEPT decrease. However, β values that ranged from ca. 8−11 $Å^{-1}$ were much smaller than what is predicted from a static tunneling model. This distance dependence is consistent with the involvement of vibrational compression along the proton transfer coordinate that accelerate CEPT and contributions from higher vibronic transitions. Furthermore, the small difference in KIE between the compounds, as well as the comparatively small E_a point to a situation where P5Q with the longest $d_{O\cdots N}$ and r_0 is the most susceptible to CEPT via higher vibronic transitions, possibly due to a more anharmonic proton potential than for the other compounds.

Fundamental studies of PCET reactions in model systems stand to impact many areas of research, e.g., for interpreting proton and hydrogen tunneling in enzymes,[5,61,64,80] or developing and optimizing the important processes of solar fuel formation, where water oxidation, CO_2 reduction, and nitrogen fixation involve complex multiple PCET processes. It has been vigorously discussed whether proton tunneling effects are important in enzmes,[81−83] and many computational approaches that serve to analyze and predict PCET reactions in enzymes and solid state catalysis ignore these effects, and instead use an adiabatic model with classical barriers.[83−85] The present study shows that proton tunneling can be very important, with rate constants varying by an order of magnitude when $d_{O\cdots N}$ varied by ∼0.3 Å. This is an important effect and a design criterion for efficient PCET catalysts. By learning how to control not only the equilibrium $d_{O\cdots N}$ value, but also the propensity for vibrational compression and involvement of higher vibronic transitions, we may be able to dramatically accelerate catalytic rates.

Because the Marcus theory of electron transfer has been present for more than half a century, there is arguably a greater understanding of how to predict and control electron transfer reactions than exists for PCET reactions. Imparting favorable electron transfer properties to the catalytic processes listed above will not necessarily ensure good catalytic activity−proton transfer must be considered as well. The theory of PCET has been developed; more fundamental and experimental studies that address how factors such as the proton tunneling distance affects PCET rates are needed to elucidate how take control of these reactions.

■ ASSOCIATED CONTENT

Supporting Information

The Supporting Information is available free of charge on the ACS Publications website at DOI: 10.1021/jacs.6b12531.

Experimental methods, temperature dependent NMR spectra and EXSY spectrum for P5Q, electrochemical methods and results, derivation of competative recombination kinetics model, summary of PCET rate constants, additional correlation plots, derivation of the relationship between $\Delta G°$ and $\Delta G^{‡}$ for a real value of λ for an endergonic reaction, and details concerning DFT (PDF)

■ AUTHOR INFORMATION

Corresponding Authors

*sascha.ott@kemi.uu.se

*leif.hammarstrom@kemi.uu.se

ORCID

Leif Hammarström: 0000-0002-9933-9084

Present Address

†Department of Chemistry, Yale University, P.O. Box 208107, 225 Prospect Street, New Haven, Connecticut 06520−8107, United States.

Author Contributions

#S.D.G. and G.A.P. contributed equally.

Notes

The authors declare no competing financial interest.

■ ACKNOWLEDGMENTS

The authors would like to thank Dr. Andreas Orthaber for assistance with EXSY spectroscopy. Funding was provided by The Swedish Research Council (grant number 623-2011-7189, SDG; grant number 2012-4060-97215-39, LH), The Swedish Energy Agency (Project number 11674-5) and The Knut and Alice Wallenberg Foundation ("Molecular Solar Energy Sciences").

■ REFERENCES

(1) Huynh, M. H. V.; Meyer, T. J. *Chem. Rev.* **2007**, *107*, 5004−5064.
(2) Hammes-Schiffer, S.; Stuchebrukhov, A. A. *Chem. Rev.* **2010**, *110*, 6939−6960.
(3) Migliore, A.; Polizzi, N. F.; Therien, M. J.; Beratan, D. N. *Chem. Rev.* **2014**, *114*, 3381−3465.
(4) Warren, J. J.; Mayer, J. M. *Biochemistry* **2015**, *54*, 1863−1878.
(5) Hammes-Schiffer, S. *J. Am. Chem. Soc.* **2015**, *137*, 8860−8871.
(6) Barry, B. A.; Babcock, G. T. *Proc. Natl. Acad. Sci. U. S. A.* **1987**, *84*, 7099−7103.
(7) Tommos, C.; Babcock, G. T. *Biochim. Biophys. Acta, Bioenerg.* **2000**, *1458*, 199−219.
(8) Hammarström, L.; Styring, S. *Energy Environ. Sci.* **2011**, *4*, 2379−2388.
(9) Stubbe, J.; Nocera, D. G.; Yee, C. S.; Chang, M. C. Y. *Chem. Rev.* **2003**, *103*, 2167−2201.
(10) Holder, P. G.; Pizano, A. A.; Anderson, B. L.; Stubbe, J.; Nocera, D. G. *J. Am. Chem. Soc.* **2011**, *134*, 1172−1180.
(11) Minnihan, E. C.; Nocera, D. G.; Stubbe, J. *Acc. Chem. Res.* **2013**, *46*, 2524−2535.
(12) Wikström, M. K. F. *Nature* **1977**, *266*, 271−273.
(13) Sharma, V.; Enkavi, G.; Vattulainen, I.; Róg, T.; Wikström, M. *Proc. Natl. Acad. Sci. U. S. A.* **2015**, *112*, 2040−2045.
(14) Zieba, A. A.; Richardson, C.; Lucero, C.; Dieng, S. D.; Gindt, Y. M.; Schelvis, J. P. M. *J. Am. Chem. Soc.* **2011**, *133*, 7824−7836.
(15) Liu, Z.; Tan, C.; Guo, X.; Li, J.; Wang, L.; Sancar, A.; Zhong, D. *Proc. Natl. Acad. Sci. U. S. A.* **2013**, *110*, 12966−12971.
(16) Knapp, M. J.; Rickert, K.; Klinman, J. P. *J. Am. Chem. Soc.* **2002**, *124*, 3865−3874.
(17) Meyer, M. P.; Tomchick, D. R.; Klinman, J. P. *Proc. Natl. Acad. Sci. U. S. A.* **2008**, *105*, 1146−1151.
(18) Soudackov, A. V.; Hammes-Schiffer, S. *J. Phys. Chem. Lett.* **2014**, *5*, 3274−3278.
(19) Small, Y. A.; DuBois, D. L.; Fujita, E.; Muckerman, J. T. *Energy Environ. Sci.* **2011**, *4*, 3008−3020.
(20) DuBois, D. L. *Inorg. Chem.* **2014**, *53*, 3935−3960.
(21) Tarantino, K. T.; Liu, P.; Knowles, R. R. *J. Am. Chem. Soc.* **2013**, *135*, 10022−10025.

DOI: 10.1021/jacs.6b12531
J. Am. Chem. Soc. 2017, 139, 2090−2101

(22) Rono, L. J.; Yayla, H. G.; Wang, D. Y.; Armstrong, M. F.; Knowles, R. R. *J. Am. Chem. Soc.* **2013**, *135*, 17735−17738.
(23) Bourrez, M.; Steinmetz, R.; Ott, S.; Gloaguen, F.; Hammarström, L. *Nat. Chem.* **2015**, *7*, 140−145.
(24) Pappas, I.; Chirik, P. J. *J. Am. Chem. Soc.* **2015**, *137*, 3498−3501.
(25) Sun, L.; Burkitt, M.; Tamm, M.; Raymond, M. K.; Abrahamsson, M.; LeGourrièrec, D.; Frapart, Y.; Magnusson, A.; Huang-Kenez, P.; Brandt, P.; Tran, A.; Hammarström, L.; Styring, S.; Åkermark, B. *J. Am. Chem. Soc.* **1999**, *121*, 6834−6842.
(26) Lachaud, T.; Quaranta, A.; Pellegrin, Y.; Dorlet, P.; Charlot, M. F.; Un, S.; Leibl, W.; Aukauloo, A. *Angew. Chem., Int. Ed.* **2005**, *44*, 1536−1540.
(27) Mayer, J. M.; Rhile, I. J.; Larsen, F. B.; Mader, E. A.; Markle, T. F.; DiPasquale, A. G. *Photosynth. Res.* **2006**, *87*, 3−20.
(28) Markle, T. F.; Mayer, J. M. *Angew. Chem., Int. Ed.* **2008**, *47*, 738−740.
(29) Irebo, T.; Johansson, O.; Hammarström, L. *J. Am. Chem. Soc.* **2008**, *130*, 9194−9195.
(30) Johannissen, L. O.; Irebo, T.; Sjödin, M.; Johansson, O.; Hammarström, L. *J. Phys. Chem. B* **2009**, *113*, 16214−16225.
(31) Zhang, M.-T.; Irebo, T.; Johansson, O.; Hammarström, L. *J. Am. Chem. Soc.* **2011**, *133*, 13224−13227.
(32) Markle, T. F.; Rhile, I. J.; Mayer, J. M. *J. Am. Chem. Soc.* **2011**, *133*, 17341−17352.
(33) Kuss-Petermann, M.; Wolf, H.; Stalke, D.; Wenger, O. S. *J. Am. Chem. Soc.* **2012**, *134*, 12844−12854.
(34) Markle, T. F.; Tronic, T. A.; DiPasquale, A. G.; Kaminsky, W.; Mayer, J. M. *J. Phys. Chem. A* **2012**, *116*, 12249−12259.
(35) Megiatto, J. D., Jr.; Mendez-Hernandez, D. D.; Tejeda-Ferrari, M. E.; Teillout, A. L.; Llansola-Portoles, M. J.; Kodis, G.; Poluektov, O. G.; Rajh, T.; Mujica, V.; Groy, T. L.; Gust, D.; Moore, T. A.; Moore, A. L. *Nat. Chem.* **2014**, *6*, 423−428.
(36) Manbeck, G. F.; Fujita, E.; Concepcion, J. J. *J. Am. Chem. Soc.* **2016**, *138*, 11536−11549.
(37) Chen, J.; Kuss-Petermann, M.; Wenger, O. S. *J. Phys. Chem. B* **2015**, *119*, 2263−2273.
(38) Markle, T. F.; Tenderholt, A. L.; Mayer, J. M. *J. Phys. Chem. B* **2012**, *116*, 571−584.
(39) Markle, T. F.; Zhang, M.-T.; Santoni, M.-P.; Johannissen, L. O.; Hammarström, L. *J. Phys. Chem. B* **2016**, *120*, 9308−9321.
(40) Horvath, S.; Fernandez, L. E.; Soudackov, A. V.; Hammes-Schiffer, S. *Proc. Natl. Acad. Sci. U. S. A.* **2012**, *109*, 15663−15668.
(41) Kiefer, P. M.; Hynes, J. T. *J. Phys. Chem. A* **2004**, *108*, 11793−11808.
(42) Kiefer, P. M.; Hynes, J. T. *J. Phys. Chem. A* **2004**, *108*, 11809−11818.
(43) Parada, G. A.; Glover, S. D.; Orthaber, A.; Hammarström, L.; Ott, S. *Eur. J. Org. Chem.* **2016**, *2016*, 3365−3372.
(44) Parada, G. A.; Markle, T. F.; Glover, S. D.; Hammarström, L.; Ott, S.; Zietz, B. *Chem. - Eur. J.* **2015**, *21*, 6362−6366.
(45) Mayer, J. M.; Hrovat, D. A.; Thomas, J. L.; Borden, W. T. *J. Am. Chem. Soc.* **2002**, *124*, 11142−11147.
(46) Skone, J. H.; Soudackov, A. V.; Hammes-Schiffer, S. *J. Am. Chem. Soc.* **2006**, *128*, 16655−16663.
(47) Marcus, R. A. *J. Chem. Phys.* **1956**, *24*, 966−978.
(48) Marcus, R. A.; Sutin, N. *Biochim. Biophys. Acta, Rev. Bioenerg.* **1985**, *811*, 265−322.
(49) Borgis, D.; Hynes, J. T. *J. Chem. Phys.* **1991**, *94*, 3619−3628.
(50) Borgis, D.; Hynes, J. T. *Chem. Phys.* **1993**, *170*, 315−346.
(51) Borgis, D. C.; Lee, S.; Hynes, J. T. *Chem. Phys. Lett.* **1989**, *162*, 19−26.
(52) Soudackov, A.; Hatcher, E.; Hammes-Schiffer, S. *J. Chem. Phys.* **2005**, *122*, 014505.
(53) Gray, H. B.; Winkler, J. R. *Proc. Natl. Acad. Sci. U. S. A.* **2005**, *102*, 3534−3539.
(54) Wenger, O. S.; Leigh, B. S.; Villahermosa, R. M.; Gray, H. B.; Winkler, J. R. *Science* **2005**, *307*, 99−102.
(55) Weiss, E.; Wasielewski, M.; Ratner, M. *Top. Curr. Chem.* **2005**, *257*, 103−133.
(56) Edwards, S. J.; Soudackov, A. V.; Hammes-Schiffer, S. *J. Phys. Chem. A* **2009**, *113*, 2117−2126.
(57) Johannissen, L. O.; Hay, S.; Scrutton, N. S.; Sutcliffe, M. J. *J. Phys. Chem. B* **2007**, *111*, 2631−2638.
(58) Hatcher, E.; Soudackov, A. V.; Hammes-Schiffer, S. *J. Am. Chem. Soc.* **2007**, *129*, 187−196.
(59) Gilbert, M.; Albinsson, B. *Chem. Soc. Rev.* **2015**, *44*, 845−862.
(60) Perrin, C. L.; Dwyer, T. J. *Chem. Rev.* **1990**, *90*, 935−967.
(61) Hay, S.; Scrutton, N. S. *Nat. Chem.* **2012**, *4*, 161−168.
(62) Johannissen, L. O.; Scrutton, N. S.; Sutcliffe, M. J. *J. R. Soc., Interface* **2008**, *5*, 225−232.
(63) Benkovic, S. J.; Hammes-Schiffer, S. *Science* **2003**, *301*, 1196−1202.
(64) Layfield, J. P.; Hammes-Schiffer, S. *Chem. Rev.* **2014**, *114*, 3466−3494.
(65) Auer, B.; Fernandez, L. E.; Hammes-Schiffer, S. *J. Am. Chem. Soc.* **2011**, *133*, 8282−8292.
(66) Juris, A.; Balzani, V.; Barigelletti, F.; Campagna, S.; Belser, P.; von Zelewsky, A. *Coord. Chem. Rev.* **1988**, *84*, 85−277.
(67) Connelly, N. G.; Geiger, W. E. *Chem. Rev.* **1996**, *96*, 877−910.
(68) Magnuson, A.; Berglund, H.; Korall, P.; Hammarström, L.; Åkermark, B.; Styring, S.; Sun, L. C. *J. Am. Chem. Soc.* **1997**, *119*, 10720−10725.
(69) Izutsu, K. *Acid-Base Dissociation Constants in Dipolar Aprotic Solvents*; Blackwell: London, 1990.
(70) Kaljurand, I.; Kütt, A.; Sooväli, L.; Rodima, T.; Mäemets, V.; Leito, I.; Koppel, I. A. *J. Org. Chem.* **2005**, *70*, 1019−1028.
(71) Chrystiuk, E.; Williams, A. *J. Am. Chem. Soc.* **1987**, *109*, 3040−3046.
(72) To our knowledge, the pK_a of quinoline in acetonitrile has not been reported, however, the pK_a's of quinoline and pyridine in water are nearly the same (5.14 and 4.85, respectively) as reported in ref 59. We think it is reasonable to assume that the pK_a of quinoline in acetonitrile will also be very close the pK_a of pyridine in acetonitrile, which is 12.3 (ref 58).
(73) Steinfeld, J. I.; Francisco, J. S.; Hase, W. L. *Chemical Kinetics and Dynamics*, 2nd ed.; Prentice-Hall: Upper Saddle River, NJ, 1998.
(74) Kuznetsov, A. M.; Ulstrup, J. *Can. J. Chem.* **1999**, *77*, 1085−1096.
(75) Hammes-Schiffer, S.; Tully, J. C. *J. Phys. Chem.* **1995**, *99*, 5793−5797.
(76) Knapp, M. J.; Klinman, J. P. *Eur. J. Biochem.* **2002**, *269*, 3113−3121.
(77) Hodgkiss, J. M.; Damrauer, N. H.; Presse, S.; Rosenthal, J.; Nocera, D. G. *J. Phys. Chem. B* **2006**, *110*, 18853−18858.
(78) Liu, Y.; Liu, H.; Song, K.; Xu, Y.; Shi, Q. *J. Phys. Chem. B* **2015**, *119*, 8104−8114.
(79) Ludlow, M. K.; Soudackov, A. V.; Hammes-Schiffer, S. *J. Am. Chem. Soc.* **2009**, *131*, 7094−7102.
(80) Reece, S. Y.; Nocera, D. G. *Annu. Rev. Biochem.* **2009**, *78*, 673−699.
(81) Hay, S.; Scrutton, N. S. *Nat. Chem.* **2012**, *4*, 161−168.
(82) Knapp, M. J.; Rickert, K. W.; Klinman, J. P. *J. Am. Chem. Soc.* **2002**, *124*, 3865−3874.
(83) Adamczyk, A. J.; Cao, J.; Kamerlin, S. C. L.; Warshel, A. *Proc. Natl. Acad. Sci. U. S. A.* **2011**, *108*, 14115−14120.
(84) Siegbahn, P. E. M. *Acc. Chem. Res.* **2009**, *42*, 1871−1880.
(85) Nørskov, J. K.; Bligaard, T.; Rossmeisl, J.; Christensen, C. H. *Nat. Chem.* **2009**, *1*, 37−46.

DOI: 10.1021/jacs.6b12531
J. Am. Chem. Soc. 2017, 139, 2090−2101